

Synthesis of zeolitic imidazolate framework-78 molecular-sieve membrane: defect formation and elimination†

Xueliang Dong,^{ab} Kang Huang,^a Sainan Liu,^a Rufei Ren,^a Wanqin Jin^{*a} and Y. S. Lin^b

Received 25th June 2012, Accepted 6th August 2012

DOI: 10.1039/c2jm34102f

Metal–organic frameworks (MOFs) are ideal micro- and mesoporous materials for molecular separation. A defect-free MOF membrane supported on a porous substrate is required for high separation performance, however it is rather difficult to eliminate the micro-defects or intercrystalline gaps in the membranes. In this work, a ZIF-78 membrane was synthesized on a porous ZnO support. The defect formation mechanism in the membrane was illustrated by *in situ* thermal expansion analysis. A novel strategy was proposed to eliminate not only the macroscopic defects but also the intercrystalline gaps in the membrane by controlling the diffusion of solvent molecules through the channels of the ZIF-78 crystal. The ZIF-78 membrane exhibited high performance in separating H₂. The ideal selectivity and mixture separation factor of H₂–CO₂ are 11.0 and 9.5, respectively. The approach reported in this paper offers an efficient and universal strategy for the facile synthesis of high-quality MOF membranes on porous supports.

Introduction

As an extensive class of porous crystalline materials with ultra-high porosity and enormous internal surface areas, metal–organic frameworks (MOFs) have attracted considerable attention in the last decade.^{1–4} Since the initial challenge of developing MOF-based separation membranes, MOFs have been confirmed as a new generation of microporous membrane materials with a bright future.^{5–8} Recently, MOF membranes have been intensively investigated for the separation of gases (H₂, CO₂ and hydrocarbons),⁹ solvent dehydration,^{10,11} chiral resolution,¹² *etc.* More interestingly, the zeolitic imidazolate framework (ZIF, a subfamily of MOFs with zeolite like structures) membranes show promise for practical application in molecular separation because of their striking properties, such as suitable window dimensions, hydrophobic surface, and relatively high thermal and chemical stabilities.^{13,14}

Significant work on the synthesis of ZIF membranes was performed by Caro's group. They developed ZIF-7, ZIF-8, ZIF-22 and ZIF-90 membranes for the molecular sieving of H₂–gas mixtures and ethene–ethane.^{15–19} Some of these membranes showed high stability even at 200 °C and under steam. Venna and

Carreon reported a highly permeable tubular ZIF-8 membrane for CO₂–CH₄ separation.²⁰ Lai and coworkers synthesized the *c*-oriented ZIF-69 membranes for CO₂ separation from different gas mixtures.^{21,22} Their recent work focused on the effective separation of C₂–C₃ and propylene–propane by ZIF-8 membranes.^{23,24} Compared with zeolite membranes, however, the separation performances of the reported ZIF membranes have not shown obvious competitive advantages. A widely accepted explanation is the flexible frameworks or the “gate opening” effect of the ZIF crystals.²⁵ Few studies, however, attribute this result to the micro-defects in the membrane layers or crystals.

For the synthesis of ZIF membranes, organic solvents such as *N,N*-dimethylformamide (DMF) and methanol are always required. These solvents are incorporated into the cages of ZIF crystals during solvothermal synthesis. Therefore, an activating process is required to remove the solvent molecules and open up the pore structures. From the structures of ZIFs, we know that they have relatively large cages and small windows.^{13,14} The transport of the solvent molecules (especially DMF with a kinetic diameter of ~5.5 Å (ref. 26)) through the windows is not easy due to the relatively rigid imidazolate frameworks, and may induce intercrystalline defects or even cracks in the membranes and a loss of performance. Presumably, any ZIF membrane with a pore diameter or so-called window size less than the kinetic diameter of the solvent molecule will face a similar issue.

Therefore, just like the removal of templates in zeolite membranes,²⁷ the removal of organic solvents from the ZIF crystals is one of the key steps and challenges in preparing high-quality ZIF membranes. To the best of our knowledge, however, no work addressing this issue has been reported. Some

^aState Key Laboratory of Materials-Oriented Chemical Engineering, Nanjing University of Technology, 5 Xinnofan Road, Nanjing, 210009, P. R. China. E-mail: wqjin@njut.edu.cn; Fax: +86-25-8317-2292; Tel: +86-25-8317-2266

^bChemical Engineering, School for Engineering of Matter, Transport and Energy, Arizona State University, Tempe, AZ 85287, USA

† Electronic supplementary information (ESI) available: H₂–CO₂ separation performance of the representative MOF membranes and polymeric membranes. See DOI: 10.1039/c2jm34102f

researchers, aware of the importance of this process, developed a water system for the synthesis of a ZIF-8 membrane.^{23,24} Unfortunately, most ZIFs cannot follow such a synthesis process because of the low solubility of imidazolate ligands in water.

In this paper a typical ZIF material, ZIF-78²⁸ with a GME topology, is used for the synthesis of high quality ZIF membranes using DMF solvent. The cage size in ZIF-78 is 7.1 Å and the window size is 3.8 Å. The integrated ZIF-78 membrane is prepared *via* a robust MOF membrane preparation method, namely reactive seeding, which was developed in our previous work.¹⁰ This is the first time that this approach has been applied to the preparation of ZIF membranes. The relationship between the removal of DMF and defect formation in the ZIF-78 membrane is illustrated. A novel effective strategy is proposed to eliminate the defects. The prepared ZIF-78 membrane shows high performance in hydrogen separation.

Experimental

Preparation of the ZnO support

ZnO powders (particle size of *ca.* 1 μm) were uniaxially pressed at 200 MPa to prepare disks with a diameter of 28 mm and thickness of 2 mm. The disks were then sintered at 645 °C for 2 h to form a porous support with an average pore size of *ca.* 100 nm and a porosity of about 30%. One side of the support was polished with SiC sandpaper, washed in deionized water, and dried before being used for the growth of the ZIF membrane.

Synthesis of the ZIF-78 powder

A mixture of Zn(NO₃)₂·6H₂O (0.238 g, 0.8 mmol), 2-nitroimidazole (nIm, 98.5%, 3B Scientific Corporation, 0.113 g, 1 mmol), 5-nitrobenzimidazole (nbIm, 98%, Alfa Aesar, 0.163 g, 1 mmol), and dimethylformamide (DMF, 28 ml) was stirred for 30 min to form a homogeneous solution. The solution was then placed in an autoclave (45 ml) and maintained at 120 °C for 24 h. After cooling, the solution was centrifuged. ZIF-78 powders were obtained after the precipitates were washed with DMF and dried.

Preparation of the ZIF-78 membrane

A typical procedure for the synthesis of a ZIF-78 membrane on a ZnO support by the reactive seeding method consisted of two processes. Seeding process: nIm (0.028 g, 0.25 mmol), nbIm (0.041 g, 0.25 mmol), and DMF (28 ml) were mixed and stirred vigorously for 30 min. A ZnO support was placed, with the smooth surface down, in a Teflon lined stainless steel autoclave (45 ml) with the solution mixture. The autoclave was heated to 120 °C for 12 h in an oven and then cooled down to room temperature. The support with the ZIF-78 seed layer was washed with DMF and dried. Secondary growth: the seeded ZnO support was placed into the precursor solution, with a composition of Zn(NO₃)₂·6H₂O (0.238 g, 0.8 mmol), nIm (0.113 g, 1 mmol), nbIm (0.163 g, 1 mmol), and DMF (28 ml). The autoclave, containing the seeded support and the precursor solution, was heated to 120 °C for 12 h. After cooling, the membrane was washed with DMF.

Activation of the ZIF-78 membrane

A series of methanol–DMF mixtures with different methanol concentrations of 25, 50, 75 and 100 vol% were prepared. The as-prepared ZIF-78 membrane was immersed in each of these solutions in turn for solvent exchange (12 h in each solution). The methanol exchanged ZIF-78 membrane was placed into a beaker with a small amount of methanol (the membrane was just immersed). The beaker, covered by Parafilm M laboratory film with 6 pinholes for methanol evaporation, was placed into the oven at 40 °C for 3 days. The activating process of the ZIF-78 membrane is shown in Fig. 1.

Characterization

The crystal phases of the samples were determined by X-ray diffraction (XRD) with Cu Kα radiation (Bruker, model D8 Advance). Diffraction patterns were collected at room temperature in the range of 5° ≤ 2θ ≤ 50°, with a step width of 0.05° and a scan rate of 0.2 s per step. The morphologies of the membrane and support were examined by scanning electron microscopy (SEM) (FEI, model QUANTA-200). The working parameters of the SEM were: high voltage (HV) 20–30 kV, work distance (WD) 8–10 mm and spot 2.0–3.0. The thermal expansion behavior of the ZnO support and the ZIF-78 membranes was investigated by dilatometry (Netzsch DIL 402C) with a constant heating rate of 2 °C min⁻¹ up to 150 °C in an air atmosphere. Thick ZIF-78 membranes (about 100 μm) were prepared for testing. Thermal gravimetry (TG) (STA 409 PC, Netzsch) of the ZIF-78 powder was performed in the temperature range of 25–800 °C with a heating rate of 5 °C min⁻¹ in a nitrogen atmosphere.

Single-gas permeation experiments were performed on the permeation setup as reported in our previous work.¹⁰ The permeation of small gas molecules (H₂, N₂, CH₄ and CO₂) through the activated ZIF-78 membrane and support was measured at room temperature (25 °C). The feed side was regulated at different pressures by an exactitude manometer and the permeate side was open to the atmosphere. The penetrated gas flow rate was measured by a soap film flowmeter. Ideal selectivity was calculated as the ratio of permeances.

Mixed-gas permeation experiments were performed on the permeation setup as reported in our previous work,²⁹ and the Wicke–Kallenbach mode was applied. Binary gas mixtures of

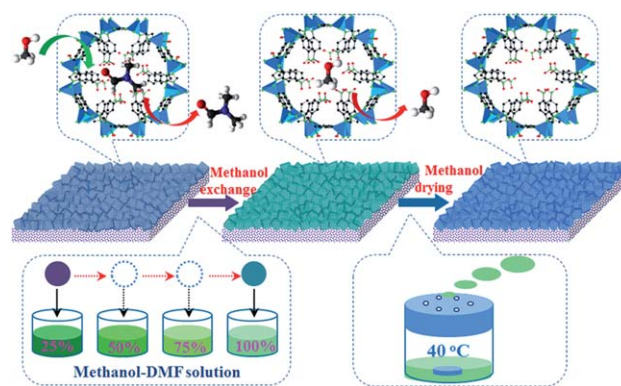


Fig. 1 Schematic diagram of the activating process of the ZIF-78 membrane.

H₂-CO₂, H₂-N₂ and H₂-CH₄ with an equal volume ratio were fed to the membrane side. The pressure at the feed side was kept at 0.15 to 0.2 MPa. Helium was used as the sweep gas and fed to the permeate side. The pressure at the permeate side was 0.1 MPa. The sweep gas was connected to an on-line gas chromatograph (Agilent 7820A) for analysis of the gas composition. The flow rates of the feed gas and sweep gas were 100 ml min⁻¹ (1 : 1) and 100 ml min⁻¹, respectively. At the steady state, the permeance (P) of component i was calculated as

$$P_i = \frac{N_i}{p_i \times A} \quad (1)$$

where N_i is the permeate rate of component i (mol s⁻¹), p_i is the trans-membrane pressure difference of component i (Pa), and A is the effective membrane area (m²).

The separation factor was calculated as

$$\alpha_{ij} = \frac{(y_i/y_j)}{(x_i/x_j)} \quad (2)$$

where x and y are the molar fractions of the component in the feed and permeate, respectively.

The selectivity was calculated as

$$s_{ij} = \frac{P_i}{P_j} \quad (3)$$

Results and discussion

By reactive seeding, the ZnO support acts as the inorganic source and reacts directly with 2-nitroimidazole (nIm) and 5-nitrobenzimidazole (nbIm) to grow a seed layer for the secondary growth. The strongly adhesive and uniform seed layer is beneficial for the preparation of a superior membrane. To confirm the feasibility of the reactive seeding method for the preparation of the ZIF-78 membrane on a porous ZnO support, the crystal structures of the seed layer and the as-prepared membrane were analyzed. As shown in Fig. 2, compared with the simulated diffraction data for ZIF-78 (Fig. 2a), the relatively weak

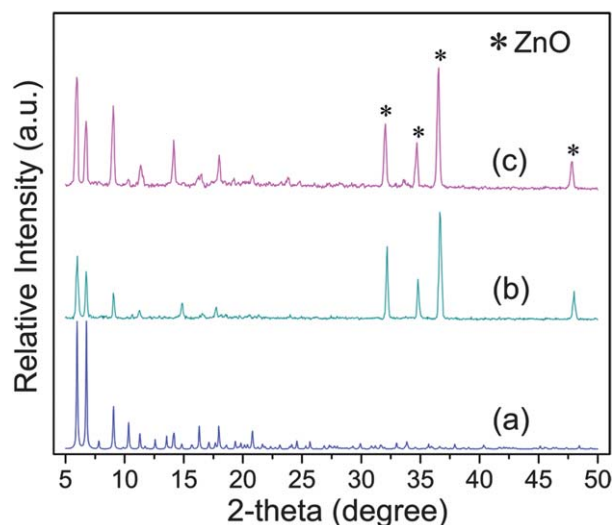


Fig. 2 XRD patterns of (a) the simulated diffraction data of ZIF-78; (b) ZIF-78 seed layer on a zinc oxide support; and (c) the as-prepared ZIF-78 membrane.

characteristic peaks of the ZIF-78 crystals can be seen clearly on the XRD pattern of the seed layer (Fig. 2b). The corresponding surface morphology (Fig. 3a) shows that regular crystal particles with a dimension of *ca.* 3 μ m are uniformly deposited on the ZnO support, indicating that a ZIF-78 seed layer has been formed *via* the reaction of nIm and nbIm with the ZnO support. From Fig. 3b, the seed layer with thickness of about 4 μ m bonded well with the support. The ZIF-78 seed layer grew into a continuous ZIF-78 membrane in the second growth step. The XRD pattern of the as-prepared membrane is shown in Fig. 2c. A full ZIF-78 phase can be observed and no obvious impurity phases are found, except for the ZnO from the support.

The as-prepared ZIF-78 membrane was activated at 100 °C and under vacuum for 12 h. For separation applications, a defect-free membrane layer deposited on a porous support is desired to achieve a high separation performance. However, many cracks are observed on the surface of the activated ZIF-78 membrane (Fig. 4a). These defects are present not only in the grain boundaries but also within the grains.

To explore the defect formation mechanism in the ZIF-78 membrane, the *in situ* expansion behavior of the as-prepared membrane was investigated. This technique is widely used for the characterization of thermal expansion of ceramic materials.^{30,31} As shown in Fig. 5, a non-linear expansion curve is observed for the as-prepared membrane. Below 105 °C, the ZIF-78 membrane gradually expands with increasing temperature, whereas it shrinks rapidly from 105–130 °C. This is due to the combined effects of thermal expansion and chemically induced volume change. Upon heating, the diffusion of large DMF molecules out of the small windows of ZIF-78 may cause the ZIF-78 crystal cell to first expand and then shrink. Most of the DMF molecules are removed at about 105 °C. This result is consistent with the TG data of the as-synthesized ZIF-78 powder (Fig. 6). A gradual weight-loss step of 6.5% up to about 100 °C can be observed. For comparison, the expansion behaviors of the activated ZIF-78 membrane and the ZnO support are also shown in Fig. 5. Almost linear thermal expansion behaviors are observed in the expansion curves of the activated membrane and the support. The expansion amount of ZIF-78 is a little larger than that of ZnO. This result further confirms that the nonlinear expansion behavior of the as-prepared ZIF-78 membrane is caused by the removal of DMF. This is the intrinsic factor that results in the cracks in the membranes.

To avoid the formation of cracks, a methanol exchange process was applied for DMF removal. The as-prepared ZIF-78 membrane was immersed in fresh methanol for 12 h and then

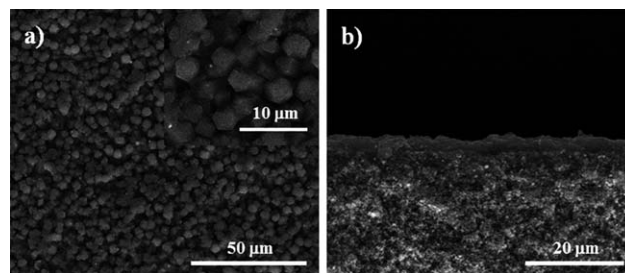


Fig. 3 SEM images of the ZIF-78 seed layer: surface (a) and cross-section (b).

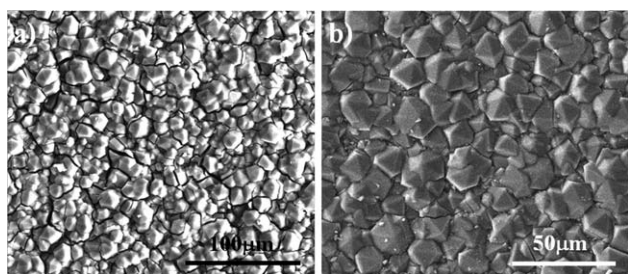


Fig. 4 SEM images of the ZIF-78 membranes activated (a) at 100 °C and under vacuum for 12 h; (b) by methanol exchange for 12 h, and then dried at 60 °C under vacuum.

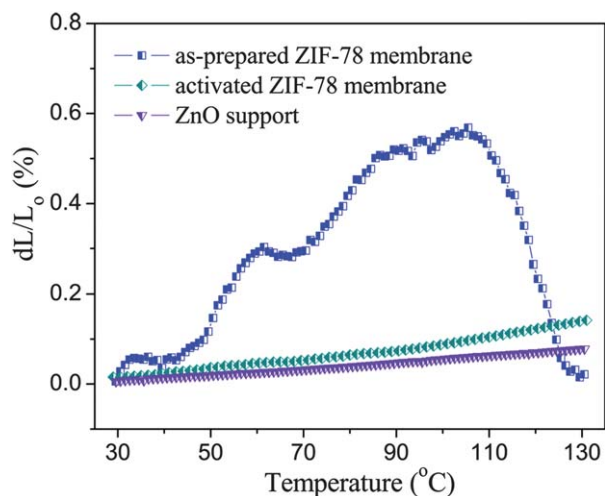


Fig. 5 Expansion behavior of the ZnO support, and the as-prepared and activated ZIF-78 membranes in an air atmosphere.

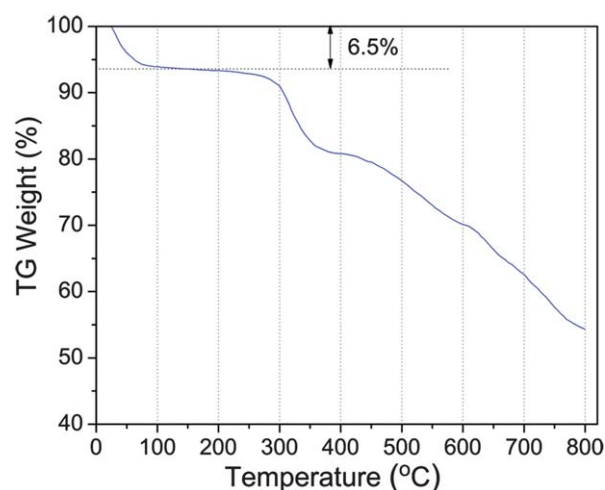


Fig. 6 TG curve of the as-prepared ZIF-78 powder.

dried at 60 °C under vacuum. However some micro-cracks could still be found on the surface of the methanol exchanged ZIF-78 membrane (Fig. 4b). This is likely due to the rapid methanol drying process.³² Therefore, the drying process of the ZIF-78 membrane was conducted at 40 °C under a nearly saturated methanol environment for 3 days (Fig. 1). On the surface of the

dry membrane, no cracks can be observed. However, we found that this membrane does not show obvious molecular-sieve behavior during the separation of small molecular gases. We think that this result is caused by intercrystalline gaps in the membranes.

Considering the difference between the heating and the methanol exchange processes for DMF removal, we find that the main difference lies in the diffusion rate of DMF through the window of ZIF-78. Obviously, a low diffusion rate is favorable for the prevention of defect formation. We speculate that, if pure methanol is used for solvent exchange, the diffusion of DMF is still too fast because of the high concentration gradient. Therefore, a series of methanol–DMF mixtures with different methanol concentrations were prepared. The as-prepared ZIF-78 membrane was immersed in these solutions in turn for solvent exchange (Fig. 1). The surface morphology of the ZIF-78 membrane activated by this optimized procedure (controlled solvent exchange and drying process) is shown in Fig. 7a and b. The membrane is orange, and the surface is homogeneous, free of cracks and covered by truncated hexagonal prismatic grains with an average size of about 20 μm. A high degree of intergrowth of the grains within the ZIF-78 membrane is observed. Fig. 7c illustrates that the ZIF-78 layer is well bonded with the ZnO support, and the thickness of the membrane is about 25 μm.

To further assess the integrity of the ZIF-78 membranes, the permeances of single small gas molecules (H_2 , CO_2 , N_2 , CH_4) were measured at different trans-membrane pressure drops (TMP). The permeances of all gases are independent of the TMP (Fig. 8a), indicating the absence of macroscopic defects in the membrane. From Fig. 8a, the permeances of these small gas molecules decrease in the order $H_2 > N_2 > CH_4 > CO_2$, with increasing the molecular sizes except for CO_2 . The ideal selectivities of H_2/CO_2 , H_2/N_2 and H_2/CH_4 are 11.0, 6.6 and 6.0, respectively (Fig. 8b). The relatively low permeance of CO_2 is attributed to the strong interaction between CO_2 and ZIF-78 frameworks.³³ Banerjee *et al.*³³ stated that the two polar functional groups $-NO_2$ in ZIF-78 make it show the highest affinity for CO_2 , which has a significant quadrupole moment. As is well known, permeance is governed by both adsorption and diffusion. Although the strong interaction provides favorable adsorption of

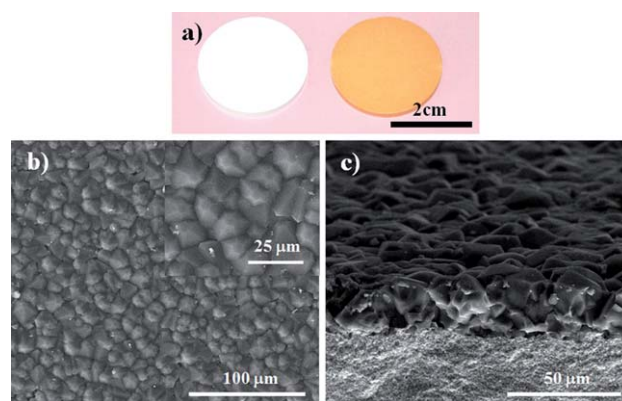


Fig. 7 (a) Digital photos of the ZnO support (left) and the activated ZIF-78 membrane (right); SEM images of the activated ZIF-78 membrane surface (b) and cross-section (c).

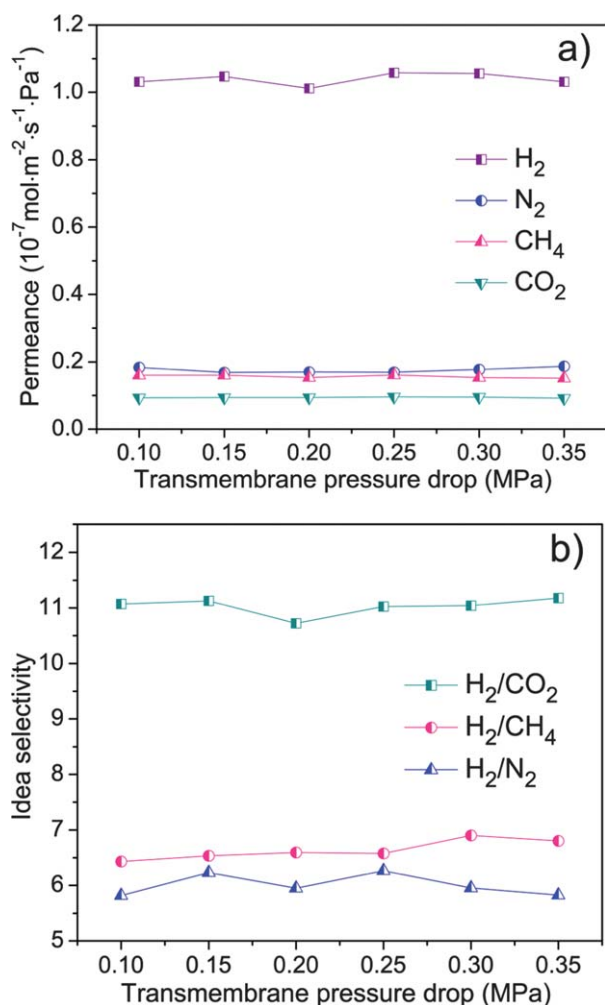


Fig. 8 (a) Single gas permeances of H_2 , N_2 , CH_4 and CO_2 through the ZIF-78 membrane as a function of trans-membrane pressure drops at 25 °C; (b) the ideal selectivities of $\text{H}_2\text{-CO}_2$, $\text{H}_2\text{-CH}_4$, and $\text{H}_2\text{-N}_2$ for the ZIF-78 membrane as a function of trans-membrane pressure drops at 25 °C.

CO_2 molecules onto the ZIF-78 membrane, it also blocks the rapid diffusion of CO_2 through the ZIF-78 channels.

In addition, the permeation behaviors of binary gas mixtures ($\text{H}_2\text{-CO}_2$, $\text{H}_2\text{-N}_2$ and $\text{H}_2\text{-CH}_4$ with an equal volume ratio) were investigated. As shown in Fig. 9, the separation factors of H_2/CO_2 , H_2/N_2 and H_2/CH_4 are 9.5, 5.7 and 6.4, respectively. All these mixture-separation factors exceed the corresponding Knudsen diffusion values. Therefore, the permeation processes of these gases through the ZIF-78 membranes follow the molecular sieving mechanism. Because of the low diffusion rate of CO_2 in the ZIF-78 channels, both H_2 and CO_2 show relatively lower permeances in the $\text{H}_2\text{-CO}_2$ system than the $\text{H}_2\text{-N}_2$ and $\text{H}_2\text{-CH}_4$ systems. It is noted that the gas permeance of the ZIF-78 membrane can be further improved by reducing the thickness of the membrane. Compared with the $\text{H}_2\text{-CO}_2$ mixed-gas separation performance of other MOF membranes, however, the ZIF-78 membrane developed in this work is among those with high separation performance (Table S1†). The Robeson plot for $\text{H}_2\text{-CO}_2$ selectivities versus CO_2 permeabilities (permeance \times membrane thickness) of polymeric membranes has been widely

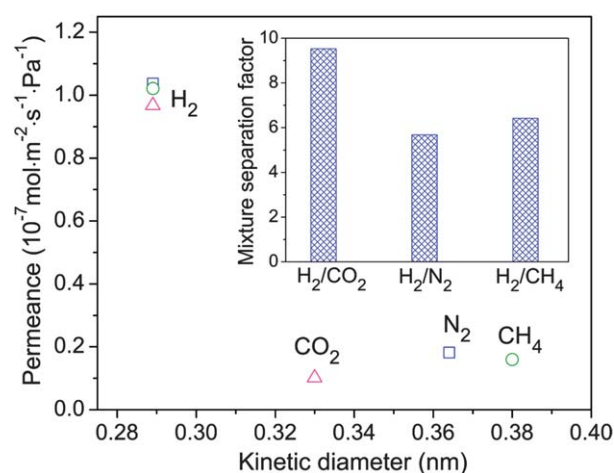


Fig. 9 Permeances of binary gas mixtures (triangles: $\text{H}_2\text{-CO}_2$, squares: $\text{H}_2\text{-N}_2$, circles: $\text{H}_2\text{-CH}_4$ with an equal volume ratio) through the ZIF-78 membranes at 25 °C as a function of molecular kinetic diameters. The inset shows the mixture separation factors for H_2 over CO_2 , N_2 and CH_4 .

used to compare the performances of membranes.³⁴ The $\text{H}_2\text{-CO}_2$ separation performance of the ZIF-78 membrane (with a H_2 permeability of 7.2×10^3 Barrer) is significantly higher than that of conventional polymeric membranes (Fig. S1†).

Conclusions

A ZIF-78 membrane is prepared for the first time *via* a reactive seeding route on a porous zinc oxide support. The support provides the metal source for the formation of the ZIF-78 seed layer. ZIF-78 membranes are easily cracked due to the non-linear expansion of the ZIF-78 layer during the solvent removal activation process. The cracks and defects can be avoided by slow exchange of the large molecule solvent with methanol in liquid state first, followed by slow drying of methanol. The ZIF-78 membrane shows molecular sieving behavior for binary mixed-gas separation and high performance especially in separating H_2 from CO_2 , with a H_2 permeability of 7.2×10^3 Barrer and a H_2/CO_2 separation factor of 9.5. This work provides a facile method to avoid the creation or enlarging of cracks and inter-crystalline defects during the activation process, which is always a necessary step for MOF membrane synthesis. Furthermore, this is a universal method, which can be widely used for the fabrication of high quality MOF crystals and MOF membranes.

Acknowledgements

This work was financially supported by the National Basic Research Program of China (no. 2009CB623406) and the National Natural Science Foundation of China (no. 21176115, no. 21006047).

Notes and references

- O. M. Yaghi, M. O'Keeffe, N. W. Ockwing, H. K. Chase, M. Eddaoudi and J. Kim, *Nature*, 2003, **423**, 705.
- S. Kitagawa, R. Kitaura and S. Noro, *Angew. Chem., Int. Ed.*, 2004, **43**, 2334.
- J. R. Li, J. Sculley and H. C. Zhou, *Chem. Rev.*, 2012, **112**, 869.

- 4 K. Sumida, D. L. Rogow, J. A. Mason, T. M. McDonald, E. D. Bloch, Z. R. Herm, T. H. Bae and J. R. Long, *Chem. Rev.*, 2012, **112**, 724.
- 5 J. Gascon and F. Kapteijn, *Angew. Chem., Int. Ed.*, 2010, **49**, 1530.
- 6 O. Shekha, J. Liu, R. A. Fischer and Ch. Wöll, *Chem. Soc. Rev.*, 2011, **40**, 1081.
- 7 A. Bétard and R. A. Fischer, *Chem. Rev.*, 2012, **112**, 1055.
- 8 D. Bradshaw, A. Garai and J. Huo, *Chem. Soc. Rev.*, 2012, **41**, 2344.
- 9 M. Shah, M. C. McCarthy, S. Sachdeva, A. K. Lee and H.-K. Jeong, *Ind. Eng. Chem. Res.*, 2012, **51**, 2179.
- 10 Y. X. Hu, X. L. Dong, J. P. Nan, W. Q. Jin, X. M. Ren, N. P. Xu and Y. M. Lee, *Chem. Commun.*, 2011, **47**, 737.
- 11 J. P. Nan, X. L. Dong, W. J. Wang and W. Q. Jin, *Microporous Mesoporous Mater.*, 2012, **155**, 90.
- 12 W. J. Wang, X. L. Dong, J. P. Nan, W. Q. Jin, Z. Q. Hu, Y. F. Chen and J. W. Jiang, *Chem. Commun.*, 2012, **48**, 7022.
- 13 K. S. Park, Z. Ni, A. P. Côté, J. Y. Choi, R. Huang, F. J. Uribe-Romo, H. K. Chae, M. O'Keeffe and O. M. Yaghi, *Proc. Natl. Acad. Sci. U. S. A.*, 2006, **103**, 10186.
- 14 A. Phan, C. J. Doonan, F. J. Uribe-Romo, C. B. Knobler, M. O'Keeffe and O. M. Yaghi, *Acc. Chem. Res.*, 2010, **43**, 58.
- 15 Y. S. Li, F. Y. Liang, H. Bux, A. Feldhoff, W. S. Yang and J. Caro, *Angew. Chem., Int. Ed.*, 2010, **49**, 548.
- 16 H. Bux, F. Y. Liang, Y. S. Li, J. Cravillon, M. Wiebcke and J. Caro, *J. Am. Chem. Soc.*, 2009, **131**, 16000.
- 17 H. Bux, C. Chmelik, R. Krishna and J. Caro, *J. Membr. Sci.*, 2011, **369**, 284.
- 18 A. S. Huang, H. Bux, F. Steinbach and J. Caro, *Angew. Chem., Int. Ed.*, 2010, **49**, 4958.
- 19 A. S. Huang, W. Dou and J. Caro, *J. Am. Chem. Soc.*, 2010, **132**, 15562.
- 20 S. R. Venna and M. A. Carreon, *J. Am. Chem. Soc.*, 2010, **132**, 76.
- 21 Y. Y. Liu, E. P. Hu, E. A. Khan and Z. P. Lai, *J. Membr. Sci.*, 2010, **353**, 36.
- 22 Y. Y. Liu, G. F. Zeng, Y. C. Pan and Z. P. Lai, *J. Membr. Sci.*, 2011, **379**, 46.
- 23 Y. C. Pan and Z. P. Lai, *Chem. Commun.*, 2011, **47**, 10275.
- 24 Y. C. Pan, T. Li, G. Lestari and Z. P. Lai, *J. Membr. Sci.*, 2012, **390–391**, 93.
- 25 C. Gücüyener, J. van den Bergh, J. Gascon and F. Kapteijn, *J. Am. Chem. Soc.*, 2010, **132**, 17704.
- 26 J. E. Elshof, C. R. Abadal, J. Sekulic, S. R. Chowdhury and D. H. A. Blank, *Microporous Mesoporous Mater.*, 2003, **65**, 197.
- 27 J. H. Dong, Y. S. Lin, M. Z.-C. Hu, R. A. Peascoe and E. Andrew Payzant, *Microporous Mesoporous Mater.*, 2000, **34**, 241.
- 28 R. Banerjee, A. Phan, B. Wang, C. Knobler, H. Furukawa, M. O'Keeffe and O. M. Yaghi, *Science*, 2008, **319**, 939.
- 29 J. P. Nan, X. L. Dong, W. J. Wang, W. Q. Jin and N. P. Xu, *Langmuir*, 2011, **27**, 4309.
- 30 X. L. Dong, Z. Xu, X. F. Chang, C. Zhang and W. Q. Jin, *J. Am. Ceram. Soc.*, 2007, **90**, 3923.
- 31 X. L. Dong, W. Q. Jin and N. P. Xu, *Chem. Mater.*, 2010, **22**, 3610.
- 32 V. V. Guerrero, Y. Yoo, M. C. McCarthy and H.-K. Jeong, *J. Mater. Chem.*, 2010, **20**, 3938.
- 33 R. Banerjee, H. Furukawa, D. Britt, C. Knobler, M. O'Keeffe and O. M. Yaghi, *J. Am. Chem. Soc.*, 2009, **131**, 3875.
- 34 L. M. Robeson, *J. Membr. Sci.*, 2008, **320**, 390.